



Mechanistic Investigation of Hydrogen Evolution Reaction from Multiple Proton Donors: The Case of Mildly Acidic Solutions Containing Weak Acids

Aria Kahyarian,¹ Alex Schumacher,² and Srdjan Nescic

Institute for Corrosion and Multiphase Flow Technology, Department of Chemical and Biomolecular Engineering, Ohio University, Athens, Ohio, USA

The present study provides a theoretical framework for mechanistic investigation of the hydrogen evolution reaction (HER) in acidic solutions containing a secondary proton donor in the form of a weak acid. The mechanistic, thermodynamic, and kinetic implications associated with the presence of a weak acid are discussed. The presence of a weak acid was shown to be able to significantly influence the polarization behavior of the HER from H^+ through its corresponding chemical dissociation reaction. This effect could lead to an increased limiting current, increased apparent Tafel slope, or even appearance of a secondary limiting current. The theoretical discussions were then applied to the case study of the HER in mildly acidic solutions containing acetic acid, on gold surface. The polarization data showed two Tafel slopes of 65 mV at lower current densities and 120 mV at higher current densities. A mechanistic mathematical model based on the initial theoretical discussions was developed and used to analyze and quantify the polarization behavior of this system. It was shown that, while in low Tafel slope range the presence of acetic acid has no effect on the HER, at 120 mV Tafel slope range the HER from acetic acid is significant, and it is occurring through a Heyrovsky type electro-desorption reaction.

© The Author(s) 2019. Published by ECS. This is an open access article distributed under the terms of the Creative Commons Attribution 4.0 License (CC BY, <http://creativecommons.org/licenses/by/4.0/>), which permits unrestricted reuse of the work in any medium, provided the original work is properly cited. [DOI: 10.1149/2.0411908jes]



Manuscript submitted December 7, 2018; revised manuscript received April 14, 2019. Published May 2, 2019. This was Paper 2034 presented at the National Harbor, Maryland Meeting of the Society, October 1–5, 2017.

The investigation of the mechanism and the kinetics of the hydrogen evolution reaction (HER) at the conditions particular to metallic corrosion in acidic media is perhaps amongst the more challenging and least discussed scenarios involving this reaction. In the context of metallic corrosion in acidic aqueous environments, the hydrogen evolution reaction can be considered as a family of cathodic reactions with molecular hydrogen as their final product.^{1–3} These reactions serve as the electron sink required for the spontaneous anodic metal dissolution reaction, and have been commonly assumed to include the reduction of hydrogen ion (H^+), as well as reduction of other weak acids such as organic acids, carbonic acid, and hydrogen sulfide.^{1,3,4} However, the presumed electrochemical mechanisms for these reactions are generally not supported with any strong experimental or analytical evidence.³

This can be in part due to the fact that the conditions commonly encountered in industrial applications, as well as academic research in this field of study, do not present an ideal setting for a detailed mechanistic investigation of the HER. The reason is the complexity arising from: mixed kinetic control, mass transfer interference, changing electrode substrate due to corrosion, fast homogeneous chemical reactions, and the presence of multiple proton donors. Some of these aspects have been addressed in previous studies by the aid of micro-kinetic models of the HER.^{5–13} These models allow for more accurate quantitative analysis of the polarization behavior under mixed kinetics resulting from the alternating rate determining step, or when multiple reaction routes are in play simultaneously.^{5,6,11} Furthermore, the effect of mass transfer from the bulk solution and the local deviations in surface concentration of H^+ or other (electro)chemical active species are also included in calculations to provide more comprehensive models.^{10–13} Amongst various approaches in micro-kinetic modeling of the HER, the adaptation of Newman's approach¹⁴ in modeling the electrochemical systems provides the flexibility required for more generic discussions. Even though they are computationally demanding, these models can be readily adopted to various hydrodynamic conditions, expanded to include complex homogeneous chemical systems and absorb the complexity arising from numerous elementary steps and multiple adsorption/desorption sites. All with maintaining detailed mechanistic description of the underlying physicochemical processes and using

minimal conditional assumptions. Such a comprehensive and flexible computational approach is of great interest in the present study, which is focused on the mechanistic implications of the HER from multiple proton donors due to the presence of a weak acid in the solution.

The significant effect of weak acids on polarization behavior of the HER reaction has been known for decades. The increased limiting currents in a buffered solution was reported by Hurlen et al. in 1984¹⁵ and associated with a CE reaction mechanism due to the presence of the weak acid. Similar mechanism is repeatedly used to explain the increased limiting currents of the HER in acidic buffered systems in the literature.^{12,16–22} Furthermore, the presence of two peak currents for some weak acids in specific pH ranges has been reported and associated with a similar CE mechanism.^{12,17,23,24} The presence of two current peaks is known to be influenced by the nature of the weak acid (pKa) and the pH at the vicinity of the electrode surface.^{12,17,23} In such scenario, when the pH at the vicinity of the electrode surface reaches a high enough value under mass transfer limitation of H^+ , the dissociation of the weak acid becomes favorable. This process results in the observation of a second peak current at more negative potentials.

On the other hand, following the example of HER from direct reduction of water, in other reports the increased limiting currents as well as the observation of two current peaks in the presence of weak acids was frequently associated with the direct reduction of weak acids rather than the abovementioned CE mechanism.^{3,4,25–30} In some early studies, even a EC' (catalytic) mechanism was proposed that implied the HER is occurring mainly via electrochemical reduction of the weak acid (carbonic acid in this case^{31,32}) followed by association of the conjugate base (bicarbonate ion) with H^+ .^{31,32} In other cases, the presence of a secondary peak current was readily associated with the direct reduction of the involved weak acid, e.g. for the case of hydrogen sulfide,^{26,27,33} and the case of sulfuric acid.³⁴ Even though the deficiencies of some of the abovementioned arguments are now understood,^{1–3,21,22} the direct electrochemical reduction of weak acids remain a valid possibility that needs to be considered alongside their chemical activity in mechanistic and quantitative discussions.

This investigation is an attempt to develop a comprehensive and generic theoretical framework for mechanistic investigations of the HER in such systems. In the following sections, first the possible effects of weak acids, as a secondary proton donor, on the HER in acidic solutions is theoretically discussed. The second part of the manuscript is a case study that demonstrates how this theoretical discussion can be used for analysis of the polarization curves associated with the HER

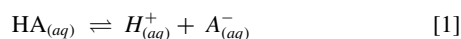
*Electrochemical Society Member.

²E-mail: ak702711@ohio.edu

in acidic solutions, and to ultimately extract mechanistic information from them. The discussion in that part covers the case of hydrogen evolution in mildly acidic solutions containing acetic acid and sodium chloride, on a gold surface.

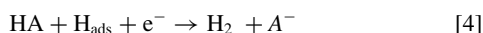
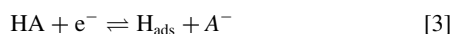
Theoretical Background on HER in Presence of a Weak Acid

By definition, a weak acid (HA in this discussion) is only partially dissociated in aqueous acidic solutions as shown by Reaction 1. Therefore, the undissociated and the dissociated forms are concurrently present, while their relative concentration is defined by the dissociation equilibrium as shown in Equation 2. Hence, the HER could possibly occur both from reduction of the H^+ and the direct reduction of the undissociated weak acid.

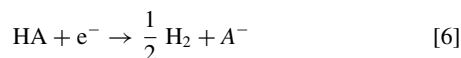


$$K_{HA} = \frac{C_{H^+} C_{A^-}}{C_{HA}} \quad [2]$$

The hydrogen evolution reaction is most commonly described for the case of H^+ by the set of three elementary reaction steps known as the Volmer step, the Heyrovsky step, and the Tafel step. However, depending on the electrode composition and environmental conditions, other elementary steps such as surface diffusion or another based on H_2^+ intermediate species have also been proposed in the literature.^{13,35,36} The mechanism of the HER from weak acids such as water (H_2O), organic acids, carbonic acid (H_2CO_3), and hydrogen sulfide (H_2S) are also described by analogous elementary steps. Using a generic formulation, these elementary steps can be expressed through Reactions 3 to 5, where HA represents the proton donor (such as H^+ , H_2O , HAc, H_2CO_3 , H_2S , etc.) and A^- represents the corresponding conjugate base. Here, in order to limit the present discussion to cathodic reactions, the reverse reaction – hydrogen oxidation – was assumed to be insignificant.



The overall HER mechanism can be seen as a combination of these elementary steps, where the net cathodic reaction can be expressed as:



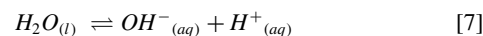
Even though the overall reaction is always the same, the rate of HER reaction is defined by the kinetics of the rate determining step. Hence, the kinetics of this reaction and its potential and pH dependence may vary dramatically depending on the governing mechanism. That denotes the significance of mechanistic studies when attempting to quantify and predict the rates of these electrochemical reactions.

Conventionally, one of the main tools in mechanistic investigation of the HER is the analysis of the characteristic kinetic parameters such as Tafel slope and reaction order obtained from steady state polarization data.^{37–41} These parameters are experimentally obtained by measuring the change in the current as a function of potential (for Tafel slope) and a function of pH or other species in solution (for reaction order). The mechanism of the HER at various conditions is determined by identifying a reaction sequence where theoretical kinetic parameters match the experimental values best. The theoretically calculated characteristic parameters are usually determined based on simplified kinetic rate expressions, at certain limiting conditions.^{36,40,42} However, these simplifying assumptions greatly limit the validity range of the resulting theoretical discussions. Additionally, they do not provide any insight for more elaborate scenarios like, the case of mixed kinetics (multiple reaction pathways), the effect of solution chemistry

in presence of weak acids, or the case of the transition from one rate-determining step to another. Such deficiencies may result in misinterpretation of the experimentally obtained characteristic parameters.

The present study develops a theoretical framework for interpretation of the polarization behavior of the HER in the more elaborate scenario of hydrogen evolution from multiple proton donors. The following sections provide a theoretical discussion on the plausible ways that the presence of a weak acid could influence the charge transfer processes of the HER in acidic solution.

Water chemistry.—In an aqueous solution containing a weak acid, the two homogeneous reactions are the weak acid dissociation shown by Reaction 1, and water dissociation as shown by Reaction 7.



$$C_{OH^-} C_{H^+} = K_w \quad [8]$$

The chemical equilibria corresponding to the weak acid and water dissociation can be mathematically expressed as Equation 2 and Equation 8, respectively. In addition to the chemical equilibria, the ionic speciation also needs to satisfy the electro-neutrality constraint as shown by Equation 9:

$$\sum_i z_i C_i = 0 \quad [9]$$

The solution speciation is defined by the chemical equilibria and the electro-neutrality equation at any given pH and concentration of the weak acid. However, since weak acids partially dissociate in an aqueous solution, the concentration of the undissociated weak acid is usually not known explicitly. Instead, the initial amount (i.e. the total amount) of weak acid is commonly known (C_{sum}), which is the sum of the undissociated weak acid (HA) and its corresponding dissociated anion (A^-). This can be expressed in terms of mass conservation for the anion as Equation 10.

$$C_{sum} = C_{HA} + C_{A^-} \quad [10]$$

Considering the equilibrium relationship of the weak acid (Equation 2) along with Equation 10, it can be readily seen that the fraction of the weak acid in its undissociated form is directly related to the acidity of the solution as shown in Equation 11. That suggests at more acidic solutions, the weak acid tends to remain in its undissociated form, while in less acidic solutions the dissociate form becomes thermodynamically more favorable.

$$\frac{C_{sum}}{C_{HA}} = 1 + \frac{K_{HA}}{C_{H^+}} \quad [11]$$

Thermodynamic feasibility of the HER from a weak acid.—The thermodynamics of the HER reaction from a weak acid, HA, according to Reaction 6, can be discussed based on the Nernst Equation:

$$E_{rev,HA} = E_{HA}^\circ - \frac{RT}{nF} \ln \left(\frac{p_{H_2}^{0.5} C_{A^-}}{C_{HA}} \right) \quad [12]$$

For the case of HER from weak acids, the concentration of the undissociated weak acid and its corresponding anion are bound by the chemical equilibrium, shown via Equation 2. Hence, the Nernst equation describing the reversible potential of the HER from a weak acid can be stated as Equation 13, which incorporates the chemical equilibrium of the weak acid. Considering that the first two terms on the right hand side are defined based on the standard Gibbs free energy of the involved species, their difference can be shown to be equal to $E_{H^+}^\circ$. Hence, $E_{rev,HA} = E_{rev,H^+}$.

$$E_{rev,HA} = E_{HA}^\circ - \frac{RT}{nF} \ln(K_{HA}) - \frac{RT}{nF} \ln \left(\frac{p_{H_2}^{0.5}}{C_{H^+}} \right) \quad [13]$$

The treatment above leads to the conclusion that the thermodynamic feasibility of HER from any given weak acid is identical to

that of H^+ ion reduction reaction. Since the above discussion does not include any specific assumptions, this conclusion is universal and is valid in all acidic solutions and for all weak acids. Therefore, the HER reaction from different weak acids is thermodynamically feasible whenever the H^+ reduction is occurring. That leaves the kinetics of charge transfer reactions as the only means of differentiating these two processes.

Kinetics of the HER in presence of a weak acid.—As discussed in more details in our earlier study,¹³ the rate of each elementary step (Reaction 3 to Reaction 5) can be expressed via Equations 14 through 16, respectively.

$$\nu_{V,H^+} = k_{f,V,H^+} (1 - \theta) C_{H^+} e^{-\lambda_{V,H^+} u \theta} e^{-\beta_{V,H^+} \frac{FE_{app}}{RT}} - k_{b,V,H^+} \theta e^{(1-\lambda_{V,H^+}) u \theta} e^{(1-\beta_{V,H^+}) \frac{FE_{app}}{RT}} \quad [14]$$

$$\nu_{H,H^+} = k_{f,H,H^+} C_{H^+} \theta e^{(1-\lambda_{H,H^+}) u \theta} e^{-\beta_{H,H^+} \frac{FE_{app}}{RT}} \quad [15]$$

$$\nu_T = k_{f,T} \theta^2 e^{2(1-\lambda_T) u \theta} \quad [16]$$

In the equations above, the symbol k stands for the reaction rate constant, θ is the surface coverage by adsorbed hydrogen atoms (H_{ads}). The first exponential terms describes the effect of interaction between H_{ads} on the surface where u is the correlation coefficient of the change in Gibbs free energy of adsorption, and whenever present, the second exponential term accounts for the effect of potential with E_{app} being the applied potential with reference to the standard hydrogen electrode. It should be noted that the standard potential term as a constant value parameter is lumped with the reaction rate constant in the above relationships. The current density corresponding to each reaction route is calculated based on: $i_j = n_{net} F \nu_j$, for each rate determining step j , with n_{net} being the total number of electrons transferred in each route, and F being the Faraday's constant.

When a weak acid is present, two additional elementary steps are plausible and should be included to account for the HER from the weak acid: a Volmer type electro-adsorption of H_{ads} from the weak acid in form of Reaction 3, and a Heyrovsky type electro-desorption in from of Reaction 4. The elementary steps which only involve the adsorbed hydrogen atoms as reactants (e.g. the Tafel step) are not directly affected by the presence of the weak acid and remain unchanged. The rates of reactions associated with the presence of the weak acid (HA) can therefore be expressed via Equations 17 and 18, for Volmer and Heyrovsky type reactions, respectively.

$$\nu_{V,HA} = k_{f,V,HA} (1 - \theta) C_{HA} e^{-\lambda_{V,HA} u \theta} e^{-\beta_{V,HA} \frac{FE_{app}}{RT}} - k_{b,V,HA} \theta C_{A^-} e^{(1-\lambda_{V,HA}) u \theta} e^{(1-\beta_{V,HA}) \frac{FE_{app}}{RT}} \quad [17]$$

$$\nu_{H,HA} = k_{f,H,HA} C_{HA} \theta e^{(1-\lambda_{H,HA}) u \theta} e^{-\beta_{H,HA} \frac{FE_{app}}{RT}} \quad [18]$$

The reaction rate expressions defined above serve as the basis of the discussion in the following sections and are able to describe various mechanistic scenarios depending on the values of the physiochemical constants such as reaction rate constant k , correlation coefficient u , and transfer coefficients β and λ . It should be noted that, when needed, the rate of other elementary reactions such as those involving H_2^+ or surface diffusion step¹³ (included in the model developed in the following case study section), can be expressed in the same fashion to those above.

As it appears from reactions 14 to 18 and their corresponding rate expressions, the HER from the H^+ and the weak acid are inter-related and the mechanism and the kinetics of these reactions may not necessarily be treated as two separate processes. The role of the weak acid in the overall reaction may vary, depending on its physiochemical properties and the catalytic behavior of the electrode surface. That is due to the coupling of the reactants, H^+ and the weak acid, through the

homogeneous chemical Reaction 1, as well as the in-common intermediate species H_{ads} . The role of the weak acid in the overall process is discussed in term of two main scenarios; first where the electrochemical adsorption of hydrogen atoms is the rate determining step, and second where the reaction rate is defined by the desorption step.

Rate determining adsorption step.—The rate determining adsorption step is the simplest mechanistic scenario for the HER, where the rate of the overall reaction is defined by the forward partial of the Volmer steps, and the surface coverage by H_{ads} is negligible. Therefore, the two reactions:



can be treated as two parallel electrochemical processes. Considering that the surface coverage by H_{ads} is negligible, the rate expressions 14 and 17, can be simplified to Equations 21 and 22 to describe the rate of the HER from each species:

$$\nu_{H^+} = k_{f,V,H^+} C_{H^+} e^{-\beta_{V,H^+} \frac{FE_{app}}{RT}} \quad [21]$$

$$\nu_{HA} = k_{f,V,HA} C_{HA} e^{-\beta_{V,HA} \frac{FE_{app}}{RT}} \quad [22]$$

As Reactions 19 and 20, and their corresponding rate expressions suggest, in this scenario the two species (H^+ and the weak acid) are acting electrochemically independent, and the net cathodic current is the sum of that from each reaction.

Rate determining desorption step.—In the case where the desorption steps are rate determining, the mechanism and the rate of reactions depend on the surface coverage of H_{ads} , as the reactant of these reactions (e.g. Tafel step). In this scenario, one can assume that the Volmer reactions are at a quasi-equilibrium state. This assumption is valid if the rate of the forward and backward partials of the Volmer reaction is significantly faster than the rate of the desorption reactions.

The presence of two parallel Volmer type reactions, one for H^+ and another for the weak acid, means that θ is defined by two quasi-equilibrium relationships. However, as discussed in the following, it can be shown theoretically that these two relationships are not linearly independent (see Appendix A). Hence, the presence of the weak acid does not affect the state of the surface coverage at a fixed pH and potential. In the case of H^+ reduction, the rate expression shown in Equation 14 can be restated for the quasi-equilibrium condition as Equation 23:

$$\frac{\theta}{1 - \theta} e^{u \theta} = K_{V,H^+} C_{H^+} e^{-\frac{FE_{app}}{RT}} \quad [23]$$

Equation 23 essentially is a Frumkin type adsorption isotherm for the surface coverage by H_{ads} , represented by θ , where K_{V,H^+} is the Equilibrium constant. The same argument applies to the Volmer reaction of the weak acid, leading to Equation:

$$\frac{\theta}{1 - \theta} e^{u \theta} = K_{V,HA} \frac{C_{HA}}{C_{A^-}} e^{-\frac{FE_{app}}{RT}} \quad [24]$$

A further examination of the rate expression as shown in Appendix A, considering the chemical equilibrium of the weak acid as expressed via Equation 2, showed that the two equilibrium constants in Equations 23 and 24 are related:

$$K_{V,HA} = K_{HA} \times K_{V,H^+} \quad [25]$$

hence:

$$K_{V,H^+} C_{H^+} = K_{V,HA} \frac{C_{HA}}{C_{A^-}} \quad [26]$$

suggesting that the two equilibrium expressions above for θ , Equations 23 and 24, are in fact identical relationships. Similar to the thermodynamic discussion, since the only assumption in above arguments is the quasi-equilibrium of Volmer type reactions, the conclusion is

universal to all acidic solutions and all weak acids. That is, the presence of a secondary proton donor in the form of a weak acid does not influence the state of hydrogen atom adsorption on the metal surface.

The discussion so far denotes that the only way for the weak acid to electrochemically contribute to cathodic currents, when the rate is limited by the desorption steps, is through a Heyrovsky type reaction. The rate of this step is defined by the surface coverage of the adsorbed hydrogen atoms as well as the concentration of the weak acid at the metal surface. In this sense, the desorption step may occur through two parallel Heyrovsky type reactions, one involving H^+ and the other involving HA.

Mass transfer and chemical reactions in presence of a weak acid.—The above discussions on the influence of the homogeneous chemical equilibria associated with the presence of a weak acid on the electrochemistry of the system signifies the importance of the solution speciation at the vicinity of the electrode surface. The surface concentrations of the chemical species when the system is influence by mass transfer or the chemical reactions are not usually known. However, the concentration distribution of the chemical species inside the boundary layer, stretching from the electrode surface to the bulk solution, is defined based on the mass conservation law through the well-known Nernst-Planck equation (Equation 27):

$$\frac{\partial C_i}{\partial t} = -\nabla \cdot N_i + R_i \quad [27]$$

The R_i term in Equation 30 reflects the effect of homogeneous chemical reactions such as weak acid and water dissociation reactions, while the flux of any given species i (N_i) is described through Equation 28.¹⁴

$$N_i = -z_i u_i F C_i \nabla \phi - D_i \nabla C_i + v_x C_i \quad [28]$$

For a one-dimensional semi-infinite geometry in the direction x normal to the metal surface, Equation 28 and Equation 27 can be simplified to Equation 29 and Equation 30 respectively, assuming a steady state and an infinitely diluted solution conditions.

$$N_i = -D_i \frac{\partial C_i}{\partial x} - \frac{z_i D_i F C_i}{RT} \frac{\partial \phi}{\partial x} + v_x C_i \quad [29]$$

$$\frac{\partial C_i}{\partial t} = 0 = D_i \frac{\partial}{\partial x} \frac{\partial C_i}{\partial x} + \frac{\partial}{\partial x} \left(\frac{z_i D_i F C_i}{RT} \frac{\partial \phi}{\partial x} \right) - v_x \frac{\partial C_i}{\partial x} + R_i \quad [30]$$

The first term in Equation 30 describes the molecular diffusion, and the second term accounts for the electro-migration of the charged species. The flux of ionic species as a result of electro-migration is defined by their concentration and the potential gradient inside the solution. The potential inside the solution can be specified by assuming that the electro-neutrality constraint (Equation 9) remains valid in the boundary layer. The effect of convective flow in the direction normal to the surface is accounted for by the $v_x C$ term, where v_x is the normal velocity component at a given distance away from the metal surface. For the laminar flow regime of the rotating disk electrode, the velocity profile and the diffusion layer thickness are obtained via Equation 31 where $a = 0.510$, and Equation 32, respectively.⁴³

$$v_x = -a\Omega \left(\frac{\Omega}{\nu} \right)^{1/2} x^2 \quad [31]$$

$$\delta = \left(\frac{3D_{lim}}{a\nu} \right)^{1/3} \left(\frac{\Omega}{\nu} \right)^{-1/2} \quad [32]$$

The rate of production/consumption of a species i through homogeneous chemical reactions (R_i in Equation 30) can be expressed in a matrix format, as Equation 33. This term incorporates the effect of the homogeneous dissociation of the weak acid in defining the speciation inside the boundary layer. As it can be seen this term is defined

by the kinetics of the reaction and does not involve a thermodynamic equilibrium assumption.

$$\begin{bmatrix} R_{H^+(aq)} \\ R_{HA(aq)} \\ R_{A^-(aq)} \\ R_{OH^-(aq)} \end{bmatrix} = \begin{bmatrix} 1 & 1 \\ -1 & 0 \\ 1 & 0 \\ 0 & 1 \end{bmatrix} \times \begin{bmatrix} k_{f,HA} C_{HA} - k_{b,HA} C_A - C_{H^+} \\ k_{f,w} - k_{b,w} C_{OH^-} - C_{H^+} \end{bmatrix} \quad [33]$$

Speciation at boundaries.—At the bulk solution ($x = \delta$) the concentrations of chemical species are constant, known values, dictated by the chemical equilibria of the solution. The concentrations of the chemical species at the metal/solution interface ($x = 0$) are defined by the rate of electrochemical reactions and their local fluxes. For an electroactive chemical species, the flux at the metal/solution boundary is equal to the superposition of corresponding electrochemical reaction rates. Therefore, for species i involved in j electrochemical reactions, the flux at the metal surface can be described through Equation 34.

$$N_i|_{x=0} = - \sum_j s_{ij} v_j \quad [34]$$

For non-electroactive species, the flux at the metal surface as a non-porous barrier is zero:

$$N_i|_{x=0} = 0 \quad [35]$$

Equation 34 and Equation 35 can be applied to describe the flux of all chemical species at the metal surface. The electric potential in the solution at the boundary may also be calculated with the aid of the electro-neutrality constraint (Equation 9).

In addition to surface concentration of the chemical species, the rate of electrochemical reactions (Equations 14 to 18) are also defined by the surface coverage of hydrogen atoms. At steady state condition, the mass conservation of adsorbed hydrogen atoms suggests:

$$\frac{d\theta}{dt} = \sum_j s_{\theta j} v_j = 0$$

With the governing equations, and the boundary conditions discussed above, the system is fully specified and may be solved to obtain the values of the unknown parameters such as aqueous concentrations of chemical species and electric potential at any point inside the boundary layer, and the surface coverage by the adsorbed hydrogen atoms.

The Effect of Homogeneous Chemical Dissociation of a Weak Acid on Electrochemical Response of the System

In investigation of the HER mechanism in solutions containing weak acids, it is crucial to separate the influence of the weak acid on H^+ reduction through its homogeneous chemical reaction from that through its electrochemical activity. With the possible contribution of the weak acid on the electrochemical processes covered earlier in this manuscript, the purpose of this section is to examine the influence of the homogeneous dissociation of a weak acid on the observed polarization behavior of the HER reaction from H^+ . In order to visualize such effects, the discussion here is developed based on the results from a comprehensive mathematical model. The model was built based on the governing physiochemical processes described earlier. In attempt to focus the present discussion on the effect of chemical dissociation of the weak acid, a simplified charge transfer scenario with a Volmer rate determining step for H^+ reduction is assumed, while the weak acid was assumed to be non-electroactive. The structure of the model and the numerical methods in use are similar to that described in detail in our earlier study, which can be used for further information.¹³

The effect of a weak acid on the polarization behavior of HER in its simplest form, is demonstrated in Figure 1. As it can be readily seen, the presence of the weak acid significantly increases the limiting current density. That is the results of the partial dissociation of the weak acid in the solution. The presence of the weak acid is expected to increase the cathodic limiting current by acting as an additional source

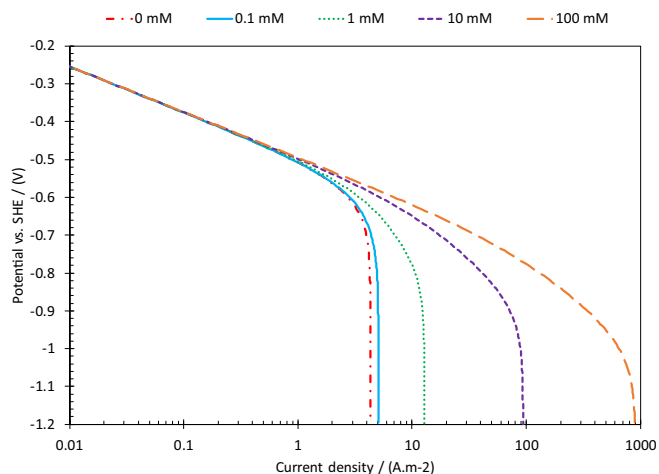


Figure 1. Simulated polarization behavior of the HER from H^+ with, Volmer rate determining step, in presence of a weak acid with $pK_a = 5$, at pH 4, $30^\circ C$, 2000 rpm RDE, and at various sum weak acid concentrations (C_{sum}).

of protons inside the boundary layer. Reaction 1 suggest that, when the surface concentration of H^+ is decreased at limiting current conditions, the equilibrium shifts toward dissociation to “buffer” the pH at the vicinity of the metal surface. The extent of this buffering ability is, of course, defined by the thermodynamic and kinetic properties of the weak acid.

Figure 2 demonstrates the effect of weak acids with various dissociation equilibrium constants on the polarization behavior of the HER at pH 4. The presence of the weak acid is shown to be able to dramatically alter the polarization behavior of the system. That is not limited to the form of an increase in limiting current as shown in Figure 1, but perhaps more importantly for this discussion, it may be in the form of deviations in the apparent Tafel slope, like that seen for a weak acid with $pK_a = 6$, or even appearance of a secondary limiting current for the case of a weak acid with $pK_a = 7$. These behaviors are due to the influence of the dissociation reaction on surface concentration of H^+ that is also noted in earlier studies.^{12,17} Weak acids with low pK_a values can readily dissociate when the surface concentration of H^+ starts to deviate from that in the bulk, as shown by Equation 11. In this case, the presence of weak acid merely results in an increased limiting current, as shown for example in Figure 1. In fact, Equation 11 suggests that the buffering action is most significant where the surface pH is close to pK_a of the weak acid. Hence, the weak acids with higher pK_a value

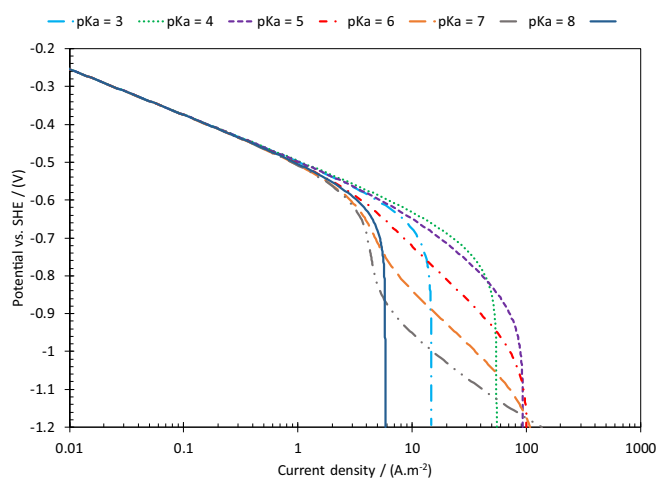


Figure 2. Simulated polarization behavior of the HER from H^+ with, Volmer rate determining step, at pH 4, $30^\circ C$, 2000 rpm RDE, $C_{sum} = 10$ mM, in presence of weak acids with varying pK_a values.

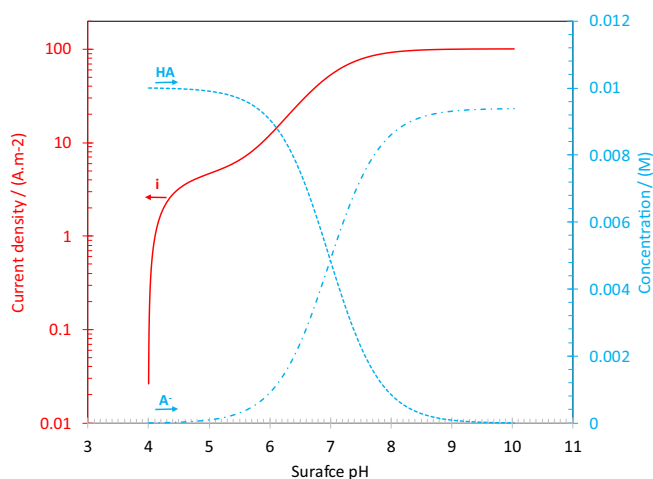


Figure 3. Calculated current density (primary vertical axes) and surface concentration of HA and A^- (secondary vertical axes) versus calculated surface pH at bulk pH of 4.0 for a weak acid with pK_a of 7 corresponding to the conditions of Figure 2.

require a higher surface pH before they have the favorable conditions to dissociate and buffer the surface pH to any significant extent. Such high surface pH values can be reached when the potential is substantially in the limiting current range. This effect may therefore appear as an increase in the apparent Tafel slope, or in more extreme cases, as a secondary limiting current, in polarization curves. This can be readily seen in the behavior of the calculated surface pH and concentrations of the weak acid and its conjugate base as shown in Figure 3. Here the dissociation of the weak acid is shown to occur only after the surface pH reaches the values close to the weak acid pK_a . At the same condition the second limiting current associated with this CE mechanism emerges in the polarization curve.

In either cases mentioned above, the cathodic current response in this range is not fully controlled by charge transfer processes, but they are also influenced by the kinetics and thermodynamics of weak acid dissociation. Additionally, the extent of these various behaviors are highly dependent on the bulk solution pH. That is, a weak acid may not exhibit any significant buffering ability in highly acidic solutions, but its presence in mildly acidic and near neutral solutions leads to appearance of secondary wave, deviation in Tafel slopes, etc. Such effects, if not carefully accounted for, may be easily mistaken with additional charge transfer processes or misinterpretation of electrochemical mechanisms that are incorrectly associated with the presence of the weak acid.

Furthermore, the increased value of limiting current with increasing pK_a of the weak acid, denotes the importance of partitioning of the weak acid to the undissociated and dissociated forms. The simulated data shown in Figure 2 is calculated for total 10mM concentration (C_{sum} in Equation 10) of any weak acid. At a given pH in the bulk solution, weak acids with relatively lower pK_a values are dissociated more than those with higher pK_a values. Therefore, the weak acids with higher pK_a values that remain in their undissociated form at bulk pH, are able to increase the limiting currents further when the surface conditions are favorable.

A Case Study: Mechanism of the HER Reaction in Mildly Acidic Solutions Containing Acetic Acid on Gold

In order to demonstrate the application of the above theoretical discussions on mechanistic investigations of the HER from multiple proton donors, a case study was considered in this section. That is, the HER in mildly acidic solutions containing acetic acid, on a gold surface, with sodium chloride supporting electrolyte. The choice of acetic acid and sodium chloride was made, as they relate to existing

Table I. Summary of the experimental conditions.

Test apparatus	Rotating disk electrode (RDE) Three electrode glass cell
Electrode material	99.99 wt% Polycrystalline gold
Rotation rate	2000 RPM
Supporting electrolyte	0.1 M NaCl
Solution Volume	1 L
Temperature	30°C
pH	2.0, 3.0, 4.0, 5.0
Total acetic acid concentration	0 mM 1.66 mM (100 ppm _m) 8.30 mM (500 ppm _m)

corrosion concerns in the oil and gas industry,^{3,4,28} hence, giving the discussion more of a practical purpose.

The mechanism of the HER from H⁺ on a gold surface was investigated in our earlier study,¹³ which is used as the foundation of the discussion here. That allowed this discussion to be focused on the effect of acetic acid, for the most part. Changing the supporting electrolyte from sodium perchlorate to sodium chloride was found to have no influence on the governing mechanism of this reaction, as discussed in the text below.

In the following, the experimentally obtained polarization data is first qualitatively analyzed. The detailed quantitative evaluation was done using a comprehensive mechanistic model developed based on the governing physiochemical laws described earlier. Using this approach, the contribution of acetic acid to the total cathodic currents was separated from that of H⁺, which allowed the mechanism of the HER from acetic acid to be determined.

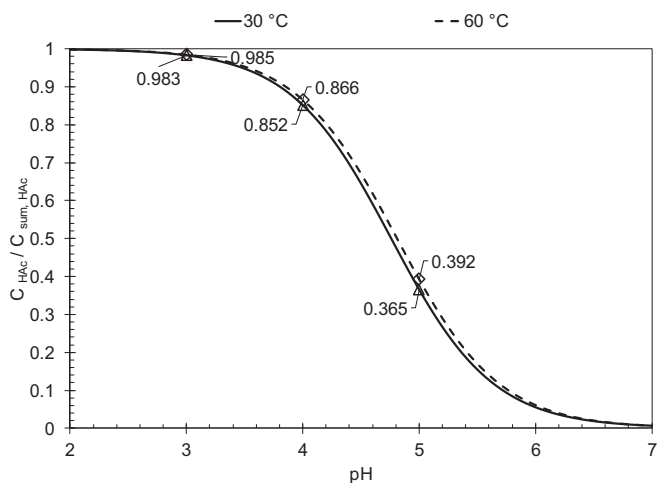
Methodology.—Experimental procedure.—The experimental apparatus and the procedures were similar to those described in an earlier publication.¹³ In the present study, the supporting electrolyte was 0.1 M solution of research grade sodium chloride in deionized water in all experiments. The targeted solution composition was achieved by addition of the desired amount of glacial acetic acid and further adjusting the solution pH using small amounts of HCl or NaOH solutions. The solution was then de-aerated using nitrogen gas for minimum of 90 min while the oxygen content of the outlet gas was monitored (Orbisphere 410). The maximum allowed dissolved oxygen content before introducing the working electrode into the solution was 1 ppb_m. The experimental conditions are summarized in Table I.

The mathematical model.—Considering the discussion in theoretical background section, the comprehensive mechanistic model developed in our earlier study for the HER in mildly acidic solutions on gold,¹³ is extended to incorporate the effect of the presence of acetic acid. This model does not have any built-in mechanistic presumptions (e.g. quasi-equilibrium) as it relates to the elementary electrochemical reactions, which makes it a universal simulation tool for the HER. Here the governing electrochemical mechanisms are formed automatically, according to the kinetic parameters obtained directly from the polarization data. Besides the presence of acetic acid, the only difference with the previous study is the use of sodium chloride supporting electrolyte instead of sodium perchlorate.

As the first step, the solution speciation was obtained for a known pH value and NaCl concentration by simultaneous solution of equilib-

rium relationships of acetic acid and water along with mass balance of acetate ion, and electro-neutrality of the solution. The equilibrium constants used here are listed in Table II. An example of the partitioning of acetic acid to undissociated form is shown in Figure 4, where the calculated ratio of $C_{HAc}/C_{sum,HAc}$ is shown at various pH values and two temperatures, 30°C and 60°C. It should be noted that, at a constant temperature the ratio $C_{HAc}/C_{sum,HAc}$ is only a function of solution pH, for example at 30°C, at pH 4 $C_{HAc}/C_{sum,HAc} = 0.8510$ and at pH 5 $C_{HAc}/C_{sum,HAc} = 0.3636$.

The mechanism of the HER on gold found in an earlier study¹³ was used as the foundation of the model developed here. There, it was shown that the HER on a gold surface follows the set of elementary steps as shown by Reactions 36 through 39.¹³ Compared to the set of generic reactions 3 to 5, the additional Reaction 37 represents the surface diffusion step, which may be limiting the rate of the Tafel reaction. It should be noted that the surface diffusion step is an inherent aspect of the HER mechanisms, which differentiates the Tafel step from the Heyrovsky step. In other words, the Tafel recombination of adsorbed hydrogen atoms requires this species to be mobile at the metal surface; a process that is represented here by the surface diffusion step. The surface diffusion step is generally assumed to be faster than

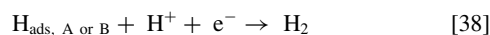
**Figure 4.** Calculated ratio of undissociated acetic acid (C_{HAc}) to total acetate ($C_{i,HAc}$) concentration at various pH values.**Table II. Equilibrium and reaction rate constants where $K = k_f/k_b$.**

Reaction rate constant	Reference
$K_{HAc} = 10^{(-\frac{1500.65}{T} - 6.50923 \times \log(T) - 0.0076792 \times T + 18.67257)}$ (M)	48
$K_w = (10^{-3} \rho_w)^2 10^{-(a_1 + \frac{a_2}{T} + \frac{a_3}{T^2} + \frac{a_4}{T^3} + (a_5 + \frac{a_6}{T} + \frac{a_7}{T^2}) \log(10^{-3} \rho_w))}$ (M^2)	
$a_1 = -4.098, a_2 = -3245.2, a_3 = 2.2362, a_4 = -3984E7, a_5 = 13.957, a_6 = -1262.3, a_7 = 8.5641E5$	49
$k_{f,HAc} = 8.7 \times 10^5$ (1/s)	50
$k_{b,w} = 1.4 \times 10^{11}$ (1/M.s)	51,52

Table III. Summary of equations used in the mathematical model.

Electrode surface boundary conditions	
$N_i _{x=0} = -\sum_j s_{ij}v_j$	for electroactive species
$N_i _{x=0} = 0$	for non-electroactive species
$\sum_i z_i C_i = 0$	
$\frac{d\theta_A}{dt} = v_{V,H^+} + v_{V,HAc} - v_{H,A,H^+} - v_{H,A,HAc} - v_D = 0$	
$\frac{d\theta_B}{dt} = v_D - v_{H,B,H^+} - v_{H,B,HAc} - 2v_T = 0$	
	Boundary layer
$\frac{\partial C_i}{\partial t} = D_i \frac{\partial}{\partial x} \frac{\partial C_i}{\partial x} + \frac{\partial}{\partial x} \left(\frac{z_i D_i F C_i}{RT} \frac{\partial \Phi}{\partial x} \right) - v_x \frac{\partial C_i}{\partial x} + R_i = 0$	for all species
$\sum_i z_i C_i = 0$	
	Bulk boundary conditions
$C_i = C_i^b$	for all species
$\Phi = 0$	arbitrary reference potential

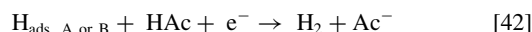
the Tafel recombination step, hence, it is not commonly included in mechanistic analyses of the HER. The particular significance of this step on the gold surface is believed to be the result of scarce low coordinated gold atoms at the surface that have a significantly high activity for Tafel recombination,^{13,44-46} as discussed in more details in the original study.¹³ In such a scenario, the surface diffusion step could be slow as compared to the Tafel step and should be included in mechanistic discussions.



In the above reactions, A and B represent two distinct reaction sites on the gold surface. As suggested by Reaction 38, the Heyrovsky reaction may occur everywhere at the surface, while the Tafel reaction is considered to be significant only on sites B. The rate relationships for Volmer, Heyrovsky, and Tafel steps can be described as discussed earlier. The rate of the surface diffusion step can be described in a same fashion, as shown in Equation 40.¹³

$$v_D = k_{f,D} \theta_A e^{(1-\lambda_D)u\theta} \quad [40]$$

In the presence of acetic acid, two additional elementary steps are plausible and should be included in order to account for the HER by direct reduction of acetic acid, according to Equations 41 and 42.



Other aspects of the model follow the discussion in the theoretical background section. The mathematical relationships used to develop this model are summarized in Table III.

HER from hydrogen ion.—The analysis of the polarization data was done in two parts. At first, the mechanism of the HER reaction from H^+ alone in a chloride containing electrolyte on a gold surface is discussed. This discussion was then used as the foundation for the second part, which is dedicated to the HER from acetic acid.

The steady state voltammograms obtained in 0.1 M sodium chloride acidic solutions at various pH values are shown in Figure 5. The cathodic polarization curves showed a similar general behavior, with currents initially increasing linearly up to the limiting current, which is associated with the charge transfer controlled hydrogen evolution from H^+ . This is followed by the mass transfer limiting current at more negative potentials, and finally another linear increase of the cathodic currents, as a result of hydrogen evolution from water. The reported current densities in Figure 5 are limited to $\sim 50 \text{ A.m}^{-2}$; a practical limit that was imposed to avoid any interference caused by the blockage effect resulting from accumulation of the evolved hydrogen gas bubbles.

The polarization behavior associated with the HER from H^+ was found to closely resemble that previously reported in perchlorate solutions,¹³ where a Tafel slopes of 65 mV, at lower current densities, and 120 mV at higher current densities, were observed. Similarly, in the pH range from 2 to 5, the apparent reaction order vs. H^+ at the lower current density range was found to be slightly below 1 (~ 0.95) as it seen in Figure 5. The similar electrochemical behavior obtained in sodium chloride and sodium perchlorate solutions,¹³ suggest that the mechanism of the HER was not affected by addition of 0.1 M chloride ions. Therefore, the same reaction mechanism can be used to describe the HER in both cases.

The kinetic parameters for elementary HER reactions from H^+ in 0.1 M NaCl solution were obtained by finding the best fit of the model to the experimental data, as shown in Figure 5. The following simplifying assumptions were used in the process:

- the interaction coefficient (u) is the same at both adsorption/desorption sites A and B;
- the effect of $H_{ads,B}$ interaction ($u\theta_B$) was assumed to be negligible considering $\theta_B \rightarrow 0$;
- all symmetry factors (β and λ) were assumed to be 0.5.

Different features of the steady state voltammograms were used to obtain the relevant physicochemical constants. The current density at which the shift in Tafel slope from 65 mV to 120 mV occurs is solely defined by the rate of the surface diffusion step, which was used to estimate $k_{f,D} = 2.0 \times 10^{-5} \text{ (mol.m}^{-2}.\text{s}^{-1})$. With the known rate constant

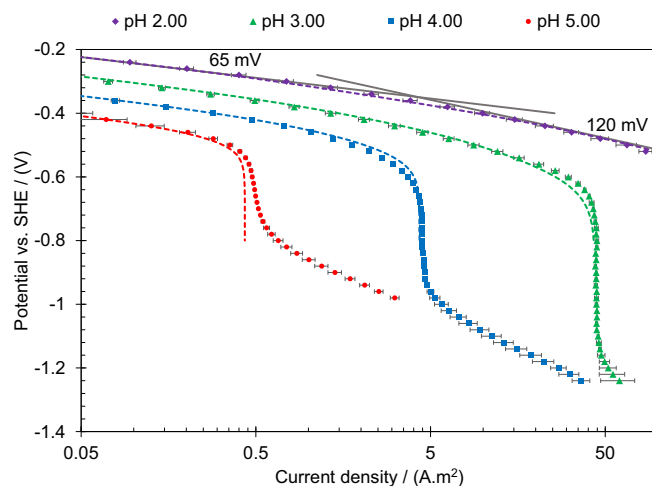


Figure 5. Cathodic steady state voltammograms obtained in 0.1 M NaCl solution, at 30°C, 2000 rpm, and pH values from 2 to 5 on polycrystalline gold surface. The points show the averaged values of at least three repeated experiments at selected potentials. Error bars show the standard deviation.

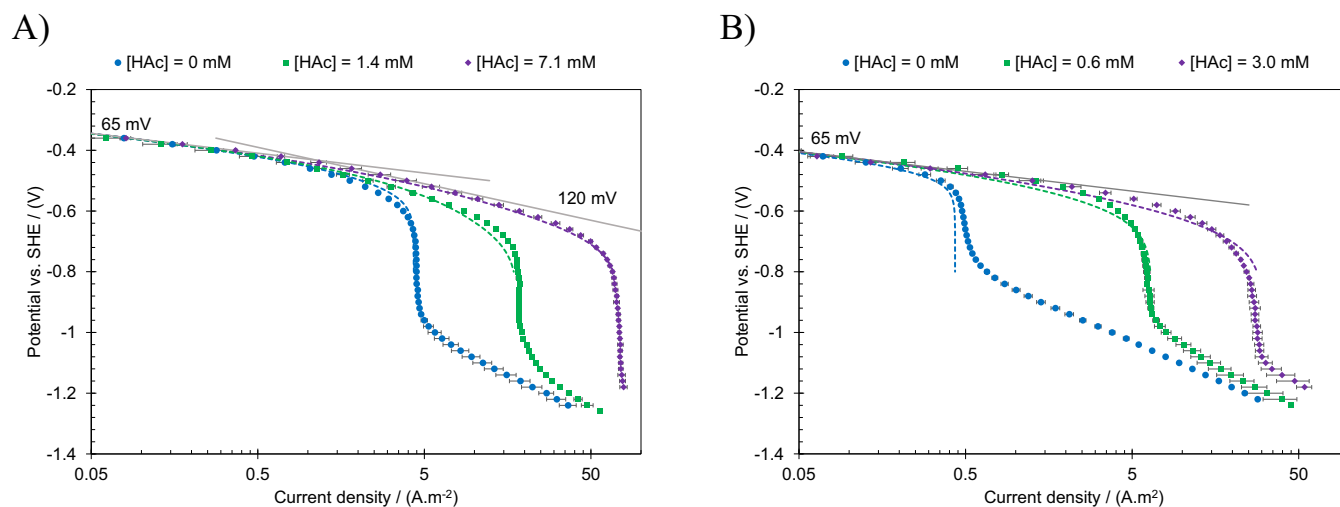


Figure 6. Cathodic steady state voltammograms obtained in 0.1 M NaCl solution, at 30°C, 2000 rpm, and $C_{t,HAc} = 0$ (blue circles), $C_{t,HAc} = 1.66$ mM (green squares), $C_{t,HAc} = 8.3$ (purple diamonds) on polycrystalline gold, at A) pH = 4 and B) pH = 5. The points show the averaged values of at least three repeated experiments at selected potentials. Error bars show the standard deviation.

of the surface diffusion step, the current density at 65 mV Tafel slope range was used to obtain the equilibrium parameters for the Volmer step. It should be noted, when the rate is defined by slow desorption steps, the steady state voltammograms do not carry any explicit information about the kinetics of the Volmer reaction. Nevertheless, the rate of the proceeding slow surface diffusion step is proportional to the magnitude of surface coverage of adsorbed hydrogen atoms (θ), which is defined by the equilibrium of the Volmer reaction as expressed by Equation 23. This criteria can be used to estimate the constants defining that equilibrium: $K_v = k_{f,v}/k_{b,v} = 5.0 \times 10^{-7} (\text{m}^3 \cdot \text{mol}^{-1})$ and $u = 3.3$. In addition, the minimum limit value of $k_{f,v} = 8.0 \times 10^{-6} (\text{m} \cdot \text{s}^{-1})$ can be estimated based on the constraint that Volmer reaction is not rate limiting in the experimental conditions considered here. These values of K_v and $k_{f,v}$ were used to obtain $k_{b,v} = k_{f,v}/K_v$.

The 120 mV Tafel slope range was used to determine the reaction rate constant of the Heyrovsky step ($k_{H,f} = 7.0 \times 10^{-10} (\text{m} \cdot \text{s}^{-1})$), considering the known values of θ from the previous steps. Additionally, the minimum limit value of the reaction rate constant for the Tafel step, $k_{f,T} = 1.0 \times 10^{-3} (\text{mol} \cdot \text{m}^{-2} \cdot \text{s}^{-1})$, was estimated by using the same considerations as described for the Volmer reaction. Since the estimated constants are implicitly coupled, the abovementioned procedure was reiterated in order to obtain the refined reported values.

The results of the model predictions, using the kinetic rate constants obtained above, were reasonably comparable to the experimental data as shown by the dashed lines in Figure 5. The model was able to properly reflect both the lower and higher Tafel slopes, while the pH dependence of the experimental polarization curves was successfully captured as well. That suggest the kinetics and the mechanism of the HER from H^+ in chloride containing solutions can be reasonably explained by the elementary steps used in developing the model (Reactions 36 through 38). Furthermore, the model also predicted the limiting current density and the mixed mass transfer/charge transfer range, with a good accuracy.

HER from acetic acid.—Considering the dominance of H^+ in more acidic solutions, the investigation of the effect of acetic acid was focused in mildly acidic solutions, where the concentration of the H^+ and undissociated acetic acid are in a reasonably comparable range. The change in the behavior of the steady state voltammograms due to the addition of acetic acid at pH 4 and pH 5 are shown in Figure 6. The addition of acetic acid significantly increased the limiting current density. As discussed above, the contribution of acetic acid to the limiting current could be through two pathways: via electrochemical reduction of acetic acid, or by buffering the H^+ concentration at

the electrode surface through homogeneous dissociation reaction (CE reaction mechanism).

The two straight lines added to Figure 6A, highlight the Tafel slopes of 65 mV and 120 mV. At lower current densities, the polarization curves in the presence of acetic acid are overlapping with the one obtained when no acetic acid was present. That suggests the addition of acetic acid did not result in any significant change of the electrochemical behavior of the system in the lower Tafel slope range. This observation accords well with the theoretical discussion of Kinetics of the HER in presence of a weak acid section. At the lower Tafel slope range, the rate is determined by a slow desorption steps, and the magnitude of θ is not affected by the presence of this species as noted in Rate determining desorption step section. Furthermore, since the slow step in this range is the surface diffusion with H_{ads} as its only reactant, the presence of acetic acid was not expected to have any significant effect on the overall rate of reaction at this range. At higher current densities with increased acetic acid concentrations, a 120 mV Tafel slope gradually emerges. The higher current densities observed in 120 mV Tafel slope range could be related to the presence of acetic acid in the solution.

At pH 5, as shown in Figure 6B, no clear secondary Tafel slope is observed. However, at low current densities, a 65 mV Tafel slope was found to fit the observed experimental behavior well. The polarization behavior of the cathodic current at lower Tafel slope range was not altered in the presence of acetic acid at pH 5, similar to what was observed at pH 4.

In order to quantify the observed electrochemical behavior shown in Figure 6, the polarization curves were analyzed initially without considering acetic acid as an electro-active species. This step was considered to examine whether the chemical dissociation of acetic acid at the vicinity of the electrode (CE mechanism) could fully explain the increased current densities. An example of the results is presented in Figure 7, showing that the magnitude of the limiting current density can be explained even if acetic acid is not considered an electro-active species. In this initial attempt, while the current densities at 65 mV range were in good agreement with the experimental data, the model failed to properly predict the polarization behavior at higher current densities. This suggests that the HER from H^+ alone even by considering the CE mechanism for acetic acid, was not sufficient to explain the steady state polarization curves. The main shortcoming is in the range of current densities associated with the Heyrovsky rate determining step. The polarization behavior at higher current density range was therefore associated with electrochemical activity of acetic acid.

As the final step, the kinetic parameters for the electrochemical contribution of HER from acetic acid and the underlying mechanism

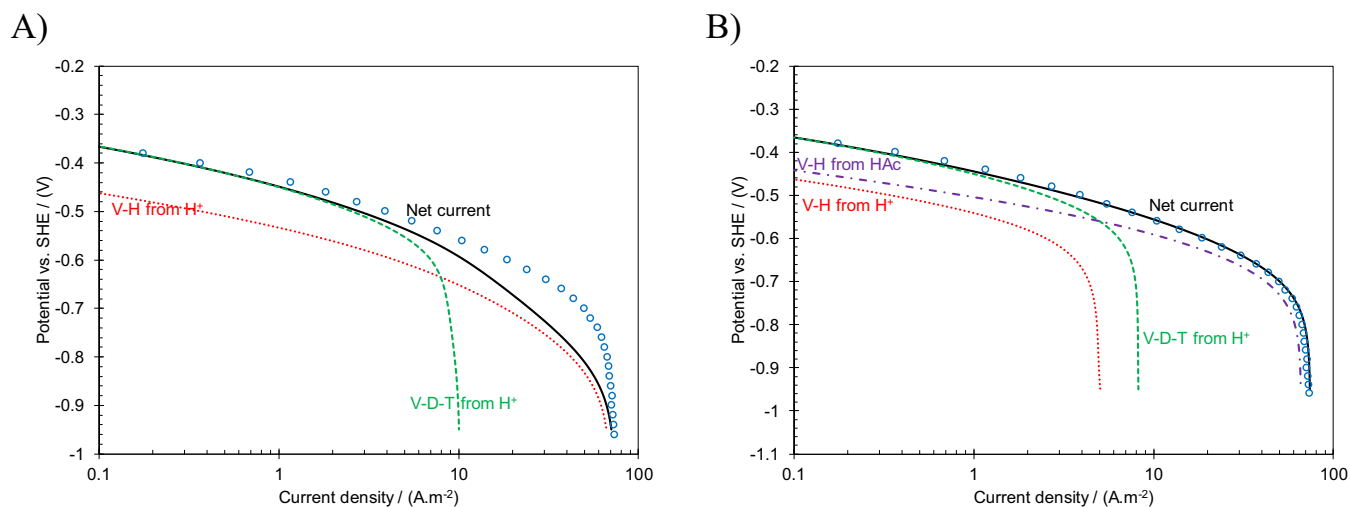


Figure 7. The illustration of the contribution of each reaction route (V-H: Volmer-Heyrovsky, V-D-T: Volmer-Diffusion-Tafel) to the net current density at pH 4, 30°C, 2000 rpm, and $C_{t,HAc} = 8.3$, undissociated acetic acid was considered A) not electroactive, B) electrochemically active. Experimental data presented as open circles.

of this reaction is determined. Considering that the HER reaction in this case study is limited by desorption steps over the whole range of cathodic currents, the kinetic constants of the Volmer type reaction from acetic acid cannot be determined from the steady state polarization data. However, the equilibrium constant of this reaction was shown to be related to that of the Volmer reaction from H^+ according to Equation 25. Hence, $K_{V,HAc} = K_{V,H^+} \times K_{HAc} = 8.75 \times 10^{-9}$ (see Appendix I for derivation). The reaction rate constant of the Heyrovsky step (Reaction 42) was obtained based on the best fit of the model to the experimental data at the 120 mV Tafel slope range ($k_{H,HAc} = 3 \times 10^{-11} \text{ (m}^3 \cdot \text{mol}^{-1} \cdot \text{s}^{-1}\text{)}$), as shown in Figure 7B.

Furthermore, the kinetic parameter obtained from this condition (Figure 7B) was used to predict the polarization behavior of the system in a wider range as shown in Figure 6. The results showed a good agreement with the experimental data. The charge transfer rates at both lower and higher Tafel slope ranges as well as the magnitude of the limiting current were predicted by the model with a good accuracy. That was considered as further validation of the mechanistic arguments above. The calculated surface coverage at both sites A and B at pH 4 and presence of acetic acid ($C_{t,HAc} = 8.3 \text{ mM}$) is shown in Figure 8. The general behavior agrees well with the results reported previously

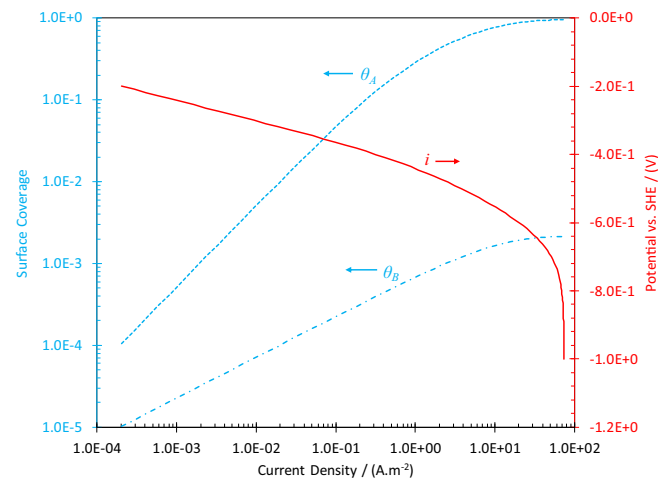
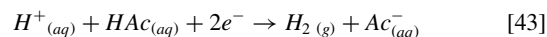


Figure 8. The calculated surface coverage at sites A and B with HAc considered to be electrochemically active at pH 4, 30°C, 2000 rpm, and $C_{t,HAc} = 8.3 \text{ mM}$.

for the case of HER in acidic solutions at lower pH values.¹³ That is a low surface coverage by H_{ads} at both A and B sites at low current densities, corresponding to the low Tafel slope range, and its gradual increase as the higher Tafel slope range is approached at more negative potentials. The population of the sites B also remains negligibly small over the whole potential range (below 0.2%).

The above mechanistic discussion suggests that the HER from acetic acid was through a Heyrovsky type recombination of adsorbed hydrogen atom with undissociated acetic acid (Reaction 42) proceeding the Volmer reaction from H^+ (Reaction 36). Therefore, the net acetic acid reduction reaction in acidic environments on gold is best represented by Reaction 43, in order to emphasize the pH dependence of this electrochemical reaction.



Reaction 43 suggests that the rate of acetic acid reduction should be sensitive to both undissociated acetic acid and H^+ concentrations. This is shown in Figure 9, where the contribution of each reaction route, calculated by the model, is presented in terms of a change in the solution pH (in Figure 9A) and undissociated acetic acid concentration (in Figure 9B). Figure 9A demonstrates the effect of changing pH from 4 to 5, while the concentration of undissociated acetic acid is constant (1.4 mM in both cases). Figure 9B shows the effect of increasing undissociated acetic acid concentration from 1.4 mM to 14 mM while a constant solution pH of 4 is maintained.

The Volmer-Heyrovsky reaction route from H^+ (blue long dashed lines) and acetic acid (red dotted dashed lines) are shown in Figure 9, which were found to behave rather similarly. At the conditions considered here, a Tafel slope of 120 mV was obtained for both routes, where for HER from H^+ with Heyrovsky rate determining step (Reaction 38) a 1.5 reaction order vs. H^+ concentration is expected.¹³ That is also observed in Figure 9A when comparing the contribution of this reaction route at pH 4 and 5. The rate of this reaction (Equation 15) is shown to be dependent on both H^+ concentration and the surface coverage of H_{ads} . Therefore, the 1.5 reaction order (vs. H^+ concentration) is a result of a direct first order dependence on H^+ concentration as the reactant, and a 0.5 order dependence on H^+ concentration through θ containing terms.

A similar behavior was observed for the HER from acetic acid through Volmer-Heyrovsky reaction route (Reaction 42). Here, the first order direct dependence on H^+ concentration in the previous case is replaced with a first order direct dependence on undissociated acetic acid concentration, as the reactant, in accordance with Equation 18. This first order dependence can be clearly observed in Figure 9B. On the other hand, the reaction rate dependence on surface coverage of

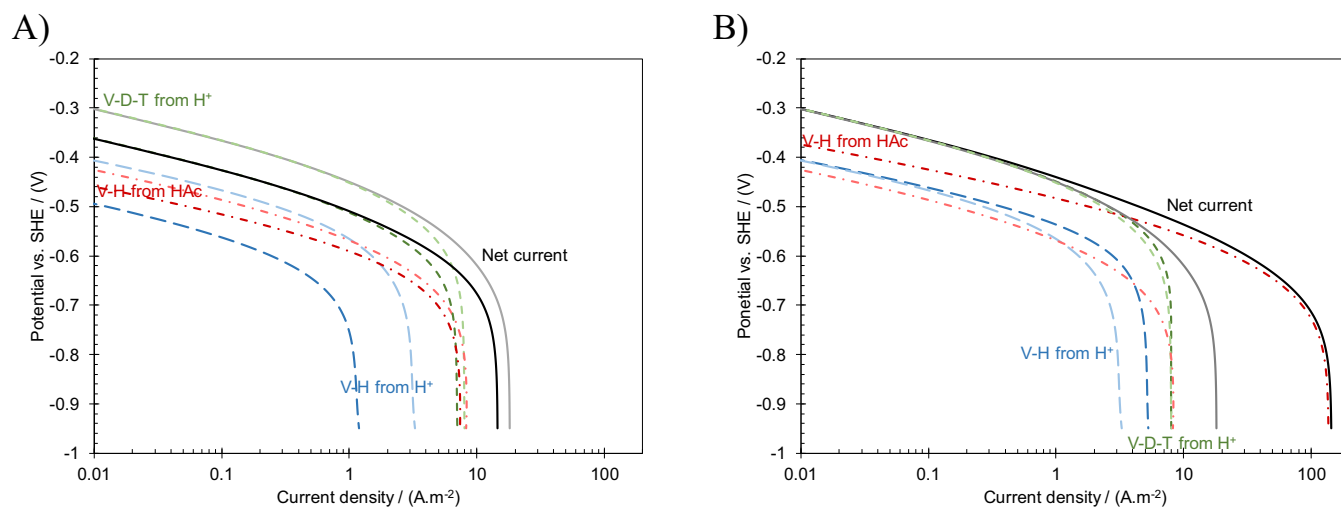


Figure 9. The rate dependence of each reaction route (V-H from H^+ : Volmer-Heyrovsky from H^+ (long dashed lines), V-D-T: Volmer-Diffusion-Tafel (Short dashed lined), Volmer-Heyrovsky from HAc (dotted dashed lines)) to the net current (solid lines) at 30°C, 2000 rpm. A) At $C_{HAc} = 1.4$ mM and pH 5 (dark shade) vs. pH 4 (light shade). B) At pH 4 and $C_{HAc} = 14$ mM (dark shade) vs. $C_{HAc} = 1.4$ mM (light shade).

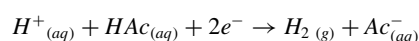
H_{ads} remains unchanged, suggesting a 0.5 order dependence on H^+ concentration through θ dependent terms. This latter pH dependence can also be observed in Figure 9A.

Conclusions

- The HER from direct reduction of a weak acid is thermodynamically identical to the HER from H^+ .
- In the context of the HER, the presence of a weak acid may lead to two additional electrochemical processes: a Volmer type electro-adsorption reaction from the weak acid, and a Heyrovsky type electro-desorption reaction involving the weak acid.
- The surface coverage by hydrogen atoms is not affected by presence of a weak acid, at any given pH and potential.
- The homogeneous chemical dissociation of a weak acid is able to significantly alter the polarization behavior of the HER from H^+ by acting as a source of H^+ at the vicinity of the metal surface. Depending on the pKa of the weak acid and the solution pH, this effect can be in the form of an increase in limiting current, increase in the observed Tafel slopes, or even appearance of a secondary limiting current.
- As a case study, the kinetics and the mechanism of the HER reaction was investigated in mildly acidic 0.1 NaCl solutions, on a polycrystalline gold surface. The analysis of polarization data showed that the governing mechanism of the HER reaction is the same as that obtained previously in sodium perchlorate solutions, suggesting that the presence of chloride in the solution up to 0.1 M did not alter the mechanism of the HER.

• In the presence of acetic acid, the analysis of the polarization curves revealed that the HER occurs from both H^+ and undissociated acetic acid, simultaneously. In the 65 mV Tafel slope range acetic acid does not significantly contribute to the cathodic currents. However, the 120 mV range was found to be dominated by the reduction of undissociated acetic acid, through a Heyrovsky type electro-desorption step.

• Considering the mechanistic discussions, the net reaction describing the cathodic reduction of acetic acid to hydrogen gas in acidic solutions is best expressed as:



Acknowledgments

The authors acknowledge the financial support from Anadarko, Baker Hughes, BP, Chevron, CNOOC, ConocoPhillips, DNV GL, ExxonMobil, M-I SWACO (Schlumberger), Multi-Chem (Halliburton), Occidental Oil Company, Petrobras, PTT, Saudi Aramco, Shell

Global Solutions, SINOPEC (China Petroleum), TOTAL, and Wood Group Kenny under a joint industrial research project.

Appendix A

The quasi-equilibrium of the Volmer reaction in the presence of a weak acid using a more fundamental treatment for expressing the charge transfer rate of a redox couple,⁴⁷ the rate of Volmer step (Reaction A1) can be expressed via Equation A2.



$$v_{V,H^+} = k_{0,H^+} \left[(1 - \theta) C_{H^+} e^{-\lambda_V u \theta} e^{-\beta V} \frac{F(E - E_0, V_{H^+})}{RT} - \psi \theta e^{(1 - \lambda_V) u \theta} e^{(1 - \beta_V) V} \frac{F(E - E_0, V_{H^+})}{RT} \right] \quad [A2]$$

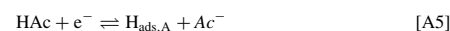
Where k_{0,H^+} is the standard reaction rate constant, E_{0,H^+} is the standard potential of Reaction A1, and ψ is the surface concentration of H_{ads} when $\theta = 1$. At quasi-equilibrium condition, the surface coverage of H_{ads} (θ) can be expressed through Equation A3, considering that $v_{V,H^+} \approx 0$.

$$\frac{\theta}{1 - \theta} e^{u \theta} = 1/\psi C_{H^+} e^{-\frac{F(E - E_0, V_{H^+})}{RT}} \quad [A3]$$

A comparison of the Equation A4 with Equation 23 shows that the adsorption equilibrium constant can be expressed as:

$$K_{V,H^+} = 1/\psi e^{\frac{FE_0, V_{H^+}}{RT}} \quad [A4]$$

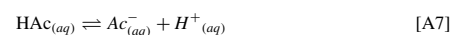
A similar treatment can be applied for the Volmer-type reaction from a weak acid, such as acetic acid in the present discussion (Reaction A5).



Assuming identical symmetry factors (λ and β) to those of H^+ , one can write:

$$v_{V,HAc} = k_{0,HAc} \left[(1 - \theta) C_{HAc} e^{-\lambda_V u \theta} e^{-\beta V} \frac{F(E - E_0, V_{HAc})}{RT} - \psi \theta C_{Ac^-} e^{(1 - \lambda_V) u \theta} e^{(1 - \beta_V) V} \frac{F(E - E_0, V_{HAc})}{RT} \right] \quad [A6]$$

Considering the chemical equilibrium of acetic acid dissociation (Reaction A7), the concentration of Ac^- can be expressed in terms of C_{H^+} and C_{HAc} based on Equation A8.



$$K_{diss} = \frac{C_{Ac^-} C_{H^+}}{C_{HAc}} \quad [A8]$$

By introducing Equation A8 into Equation A6, at quasi-equilibrium conditions, the surface coverage of H_{ads} (θ) resulting from Reaction A5, can be expressed in terms of

Equation A9.

$$\frac{\theta}{1-\theta} e^{i\theta} = \frac{1}{\psi} \frac{C_{H^+}}{K_{diss}} e^{-\frac{F(E-E_{0,V_{HAc}})}{RT}} \quad [A9]$$

Furthermore, by introducing the definition of Equilibrium constant ($K_{diss} = \exp(-\Delta G_{diss}/RT)$) and the standard potential ($E_{0,HAc} = -\Delta G_{V,HAc}/F$) based on the Gibbs free energy, a simple mathematical manipulation shows that $\exp(FE_{0,HAc}/RT)/K_{diss} = \exp(FE_{0,H^+}/RT)$. Hence, Equation A9 is simplified to that obtained for the quasi-equilibrium from H^+ (Equation A3), and:

$$\frac{1}{\psi} e^{-\frac{FE_{0,V_{HAc}}}{RT}} = K_{diss} \frac{1}{\psi} e^{-\frac{FE_{0,V_{H^+}}}{RT}} = K_{diss} \times K_{V,H^+} = K_{V,HAc} \quad [A10]$$

List of Symbols

b	Tafel slope (mV)
C_i	Concentration of species i ($\text{mol}\cdot\text{m}^{-3}$)
D_i	Diffusion coefficient of species i ($\text{m}^2\cdot\text{s}^{-1}$)
E_{app}	Applied potential (V)
F	Faraday's constant ($\text{C}\cdot\text{mol}^{-1}$)
i	Current density ($\text{A}\cdot\text{m}^{-2}$)
K_j	Equilibrium constant of reaction j (varies)
$k_{f,j}$	Forward reaction rate constant of reaction j (varies)
$k_{b,j}$	Backward reaction rate constant of reaction j (varies)
N_i	Flux of species i ($\text{mol}\cdot\text{m}^{-2}\cdot\text{s}$)
R	Universal gas constant ($\text{J}\cdot\text{mol}^{-1}\cdot\text{K}^{-1}$)
R_i	Rate of homogeneous reaction i ($\text{mol}\cdot\text{s}^{-1}\cdot\text{m}^{-3}$)
u	Correlation coefficient of H_{ads} interaction energy (unitless)
s_{ij}	Stoichiometric coefficient of species i in reaction j (unitless)
T	Absolute temperature (K)
t	Time (s)
u_i	Mobility of species i ($\text{m}^2\cdot\text{mol}^{-1}\cdot\text{s}^{-1}$)
v	Velocity ($\text{m}\cdot\text{s}^{-1}$)
x	Spatial dimension (m)
z_i	Charge of species i (unitless)

Greek

β_j	Electrochemical symmetry factor of reaction j (unitless)
δ	Diffusion layer thickness of RDE (m)
Φ	Potential in the electrolyte (V)
λ_j	Symmetry factor of reaction j due to interaction of adsorbed species (unitless)
ν	Kinematic viscosity ($\text{m}^2\cdot\text{s}^{-1}$)
Ω	Rotation speed ($\text{rad}\cdot\text{s}^{-1}$)
θ	Surface coverage of H_{ads} (unitless)
ν_j	Reaction rate of surface reaction j ($\text{mol}\cdot\text{m}^{-2}\cdot\text{s}^{-1}$)

ORCID

Aria Kahyarian  <https://orcid.org/0000-0001-8809-1493>

References

- A. Kahyarian, M. Achour, and S. Nestic, in *Trends in Oil and Gas Corrosion Research and Technologies*, A. M. El-Sherik, Editor, p. 149, Elsevier (2017).
- A. Kahyarian, M. Achour, and S. Nestic, in *Trends in Oil and Gas Corrosion Research and Technologies*, A. M. El-Sherik, Editor, p. 805, Elsevier (2017).
- A. Kahyarian, M. Singer, and S. Nestic, *J. Nat. Gas Sci. Eng.*, **29**, 530 (2016).
- S. Nešić, *Corros. Sci.*, **49**, 4308 (2007).
- M. R. Gennero de Chialvo and A. C. Chialvo, *Electrochem. Commun.*, **1**, 379 (1999).
- P. M. Quaino, M. R. Gennero de Chialvo, and A. C. Chialvo, *Electrochim. Acta*, **52**, 7396 (2007).
- M. R. Gennero de Chialvo and A. C. Chialvo, *J. Electrochem. Soc.*, **147**, 1619 (2000).
- M. R. Gennero de Chialvo and A. C. Chialvo, *Electrochim. Acta*, **44**, 841 (1998).
- A. T. Marshall, *Curr. Opin. Electrochem.*, **7**, 75 (2018).
- M. D. Arce, H. L. Bonazza, and J. L. Fernández, *Electrochim. Acta*, **107**, 248 (2013).
- H. L. Bonazza, L. D. Vega, and J. L. Fernández, *J. Electroanal. Chem.*, **713**, 9 (2014).
- M. Auinger et al., *Phys. Chem. Chem. Phys.*, **13**, 16384 (2011).
- A. Kahyarian, B. Brown, and S. Nestic, *J. Electrochem. Soc.*, **164**, H365 (2017).
- J. Newman and K. E. Thomas-Alyea, *Electrochemical Systems*, 3rd ed., Wiley-interscience, (2004).
- T. Hurlen, S. Gunvaldsen, and F. Blaker, *Electrochim. Acta*, **29**, 1163 (1984).
- K. Mikulskis, S. Kanapeckaitė, and A. Survila, *J. Electrochem. Soc.*, **165**, J3186 (2018).
- A. Survila, S. Kanapeckaitė, and K. Mažeika, *Russ. J. Electrochem.*, **54**, 33 (2018).
- C. Canhoto, M. Matos, A. Rodrigues, M. D. Geraldo, and M. F. Bento, *J. Electroanal. Chem.*, **570**, 63 (2004).
- S. Daniele, I. Lavagnini, and M. A. Baldo, *J. Electroanal. Chem.*, **404**, 105 (1996).
- A. Kahyarian, B. Brown, and S. Nestic, *Corrosion*, **72**, 1539 (2016).
- A. Kahyarian, A. Schumaker, B. Brown, and S. Nestic, *Electrochim. Acta*, **258**, 639 (2017).
- A. Kahyarian, B. Brown, and S. Nestic, *Corrosion*, **74**, 851 (2018).
- A. Kahyarian and S. Nestic, *Electrochim. Acta*, **297**, 676 (2019).
- M. Matos, C. Canhoto, M. F. Bento, and M. D. Geraldo, *J. Electroanal. Chem.*, **647**, 144 (2010).
- M. Nordsveen, S. Nešić, R. Nyborg, and A. Stangeland, *Corrosion*, **59**, 443 (2003).
- J. Kittel, F. Ropital, F. Grosjean, E. M. M. Sutter, and B. Tribollet, *Corros. Sci.*, **66**, 324 (2013).
- B. Tribollet et al., *Electrochim. Acta*, **124**, 46 (2014).
- M. B. Kermani and A. Morshed, *Corrosion*, **59**, 659 (2003).
- F. M. Song, D. W. Kirk, J. W. Graydon, and D. E. Cormack, *J. Electrochem. Soc.*, **149**, B479 (2002).
- F. M. Song, D. W. Kirk, J. W. Graydon, and D. E. Cormack, *Corrosion*, **60**, 736 (2004).
- C. de Waard and D. E. Milliams, *Corrosion*, **31**, 177 (1975).
- A. Więckowski, E. Ghali, M. Szklarczyk, and J. Sobkowski, *Electrochim. Acta*, **28**, 1619 (1983).
- Y. Zheng, B. Brown, and S. Nešić, *Corrosion*, **70**, 351 (2014).
- Y. Xiang et al., *Electrochim. Acta*, **258**, 909 (2017).
- K. Juodkazis, J. Juodkazytė, A. Grigucevičienė, and S. Juodkazis, *Appl. Surf. Sci.*, **258**, 743 (2011).
- B. E. Conway and B. V. Tilak, *Electrochim. Acta*, **47**, 3571 (2002).
- S. Schuldiner, *J. Electrochem. Soc.*, **101**, 426 (1954).
- S. Schuldiner, *J. Electrochem. Soc.*, **101**, 488 (1954).
- J. O. Bockris, I. A. Ammar, and A. K. M. S. Huq, *J. Phys. Chem.*, **61**, 879 (1957).
- J. O. Bockris and E. C. Potter, *J. Electrochem. Soc.*, **99**, 169 (1952).
- J. O. Bockris and A. K. N. Reddy, *Modern Electrochemistry: An introduction to an interdisciplinary area, Volume 2*, Plenum Press, New York, (1973).
- B. E. Conway and M. Salomon, *Electrochim. Acta*, **9**, 1599 (1964).
- W. G. Cochran, *Math. Proc. Cambridge Philos. Soc.*, **1**, 365 (1934).
- L. Stobinski, R. Nowakowski, and R. Dus, *Vacuum*, **48**, 203 (1997).
- J. A. van, B. Eveline Bus, and Jeffrey T. Miller, *J. Phys. Chem. B*, **109**, 14581 (2005).
- M. Hu, D. P. Linder, M. B. Nardelli, and A. Striolo, *J. Phys. Chem. C*, **117**, 15050 (2013).
- A. J. Bard and L. R. Faulkner, *Electrochemical methods: fundamentals and applications*, John Wiley & Sons, Inc., (2001).
- H. S. Harned and R. W. Ehlers, *J. Am. Chem. Soc.*, **55**, 652 (1933).
- W. L. Marshall and E. U. Franck, *J. Phys. Chem. Ref. Data*, **10**, 295 (1983).
- M. Eigen and E. Eyring, *J. Am. Chem. Soc.*, **84**, 3254 (1962).
- M. Eigen, *Angew. Chem. Int. Ed. Engl.*, **3**, 1 (1964).
- F. H. Stillinger, in *Theoretical Chemistry Advances and Perspectives*, H. Eyring and D. Henderson, Editors, vol. 3, p. 177, Elsevier Inc (1978).